Int. J. Solids Structures Vol. 30, No. 10, pp. 1289–1300, 1993
Printed in Great Britain

0020–7683/93 $6.00+ .00

POST-BUCKLING ANALYSIS OF MULTIPLY DELAMINATED BEAMS

IZHAK SHEINMAN and MATTI ADAN
Faculty of Civil Engineering, Technion-Israel Institute of Technology, Technion City, Haifa 32000, Israel

and

ELI ALTUS
Faculty of Mechanical Engineering, Technion-Israel Institute of Technology, Technion City, Haifa 32000, Israel

(*Received* 21 *July* 1992; *in revised form* 16 *October* 1992)

Abstract—An analytical model for the post-buckling behavior of multiply delaminated beams or long plates under cylindrical bending is presented. The model comprises partial non-linear differential equations based on the Von Karman kinematic approach. A special variable separation, based on global and local functions derived from the eigenfunction procedure, is employed to obtain the algebraic non-linear system, which is solved by the Newton–Raphson method and a modified "arc-length" procedure. Two illustrative examples are provided.

1. INTRODUCTION

One of the most serious problems associated with laminated composites is formation of multiple-delamination zones under low-velocity impact loads. It may lead to drastic deterioration in load capacity, initiated by local buckling and possibly followed by crack propagation and total failure under service load levels. Local buckling in itself does not necessarily imply the ultimate load, and usually the laminate is capable of carrying on in a post-buckling mode under higher loading. The load capacity depends heavily on the geometric interrelationship of the delaminations.

This prospect detracts from the high potential of the composites, and indicates the need for extensive research. Accordingly it has become, over the last decade, the subject of numerous publications. Most of the earlier works deal with an idealized case of single delamination in bifurcation classical buckling load (Chai *et al.*, 1981; Yin *et al.*, 1984; Simitses *et al.*, 1985; Shivakumar and Whitcomb, 1985; Sheinman *et al.*, 1989, and others). Yin (1986) and Chai *et al.* (1981) also deal with the post-buckling shape, but in terms of local delamination growth rather than of geometrical non-linear analysis. Sheinman and Soffer (1991) presented a post-buckling analysis for a composite with a single delamination, based on the geometrical model employed by Simitses *et al.* (1985) and on a finite-difference procedure, with the conclusion that the bifurcation point is indeed only an indication of the overall behavior and post-buckling analysis is called for.

A more realistic situation of multiply delaminated laminates, is considered in very few publications. Bolotin *et al.* (1980) solved the eigenproblem for a compressed simply-supported isotropic rod, centrally delaminated by a number of equally-spanned and spaced cracks. A non-linear finite-element model for the response of multiply delaminated panels under compression was developed by Chang and Kutlu (1989), with the result shown for a case of two delaminations in decoupled behavior, and no parametric study of the mutual delaminations is presented.

Recently, Larsson (1991) investigated the interaction of buckled multiply delaminated layers, concentrating on crack growth rather than on the mutual behavior of the layers in the post-buckling stage. Adan (1991) developed an analytical model for buckling problem of multiply-delaminated composite beams, with an interesting parametric study of the effect of size and relative location of the cracks.

It is apparent that the problem of multiple delaminations under impact is still open for exploration. The purpose of the present work is to investigate the effect of the mutual configuration of multiple delaminations on the overall non-linear behavior. Due to its complexity, the study is confined to the post-buckling behavior without reference to the effects of contact constraints and crack growth which, although physically an integral part of the overall pattern, can be isolated under certain conditions. The effect of contact constraints is studied separately by Adan *et al.* (1993) and will be incorporated in the present model in the future.

The one-dimensional model employed by Simitses *et al.* (1985) is extended to multiple delaminations [see Adan (1991)]. The cracks referred to as "delaminations" are assumed to exist before loading and not to grow under loading. The beam is subjected to arbitrary axial and transverse loading. The delaminations divide the beam into a sequence of regions each of which is subject to non-linear equilibrium equations. For the crack tips, displacement and force compatibility equations are imposed and finally the boundary conditions are specified. Thus, the system is composed of partial non-linear differential equations in terms of the transverse and axial displacements. For insight into the contribution of each parameter, a solution based on variable separation via function series, rather than a numerical procedure like finite differences or finite elements, was chosen. The series, composed of global and local functions derived from the eigenfunction of the delaminated beam and additional functions, satisfies the essential continuity conditions. These functions, which lead to the compatibility force condition and consequently ensure monotonic convergence, yield an algebraic non-linear system characterized by limit point behavior, which is solved by the Newton–Raphson method and a modified "arc-length" procedure.

2. ANALYTICAL FORMULATION

Kinematics

A laminated composite strip is assumed to be delaminated prior to loading by an arbitrary number of through-the-width cracks and subjected to unidirectional in-plane pressure as shown in Fig. 1(a). The delamination cracks divide the strip into m geometrically continuous regions, referred to as sublaminates [Fig. 1(b)]. A one-dimensional analytical model is employed based on the one-dimensional beam theory for small width-to-length ratios, and the cylindrical bending theory for large ones.

Assuming a small thickness-to-span (and to delamination length) ratio at which the transverse shear effect is negligible, and using the Kirchhoff–Love hypothesis, we have for each region i:

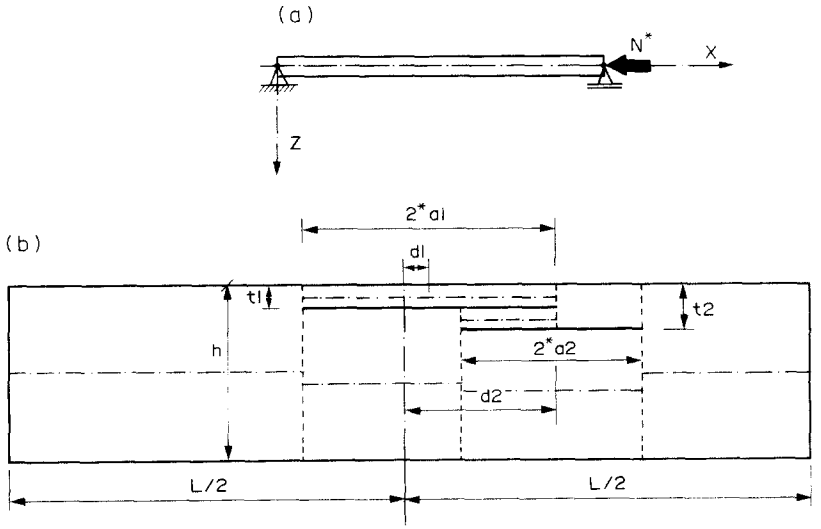

Fig. 1. Geometry, loading and sign convention.

$$U(x,z) = {}^{i}u(x,{}^{i}z_{\text{ref}}) - (z - {}^{i}z_{\text{ref}})^{i}w_{,x}(x,z_{\text{ref}}),$$
$$W(x,z) = {}^{i}w(x,{}^{i}z_{\text{ref}}), \quad i = 1,2,\ldots,m \tag{1}$$

where ${}^{i}u(x,{}^{i}z_{\text{ref}})$ and ${}^{i}w(x,{}^{i}z_{\text{ref}})$ are the axial and transverse displacements of the region's reference surface, ${}^{i}z_{\text{ref}}$ its z-coordinate and $(\ )_{,x}$ denotes differentiation with respect to the x-coordinate. Under the kinematic model, the various sublaminates may be interconnected by straight lines perpendicular to the reference axes, referred to as joints, retaining their rectilinearity and perpendicularity upon deformation. Thus the whole structure is modeled as a net of members (reference axes) and joints. For illustration purposes, characteristic partitions of the cross-section by one and two delaminations are shown in Fig. 2(a), with their schematical member-joint representation shown in Fig. 2(b). The theoretical singularity at the crack tips, and the plasticity effect which may occur, are not taken into account. At moderately small rotation, the Von Karman strain and change of curvature of the reference surface associated with the displacement field (u, w) and imperfection function ${}^{i}\bar{w}$, are:

$$ {}^{i}\varepsilon_{xx}(x,{}^{i}z_{\text{ref}}) = {}^{i}u_{,x} + \tfrac{1}{2}{}^{i}w_{,x}({}^{i}w_{,x} + 2{}^{i}\bar{w}_{,x}),$$
$$ {}^{i}k_{xx}(x,{}^{i}z_{\text{ref}}) = -{}^{i}w_{,xx}. \tag{2}$$

Constitutive equations

Under the one-dimensional beam theory (small width-to-span ratio), the force–strain relation can be reduced to

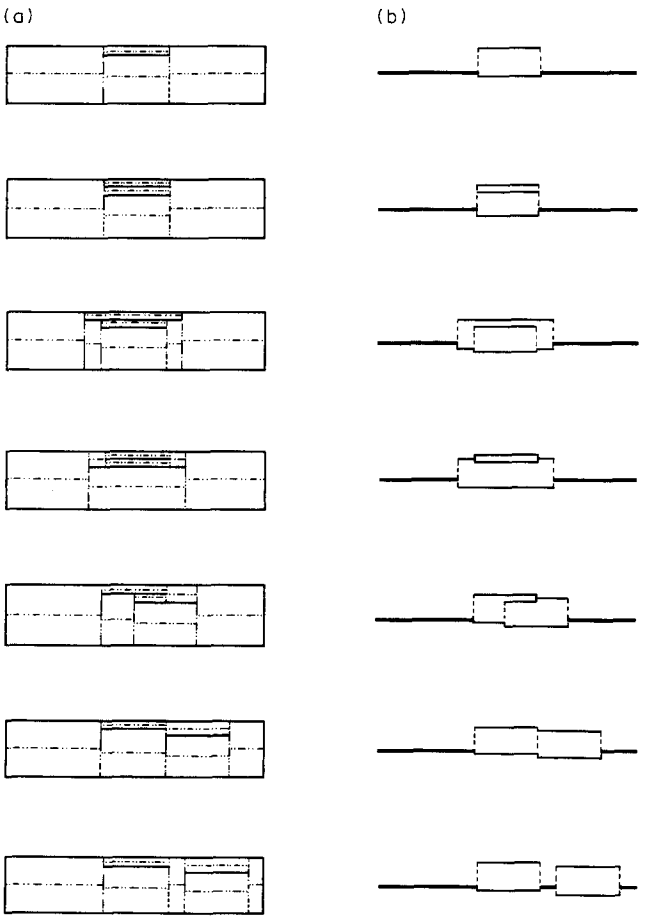

Fig. 2. Various configurations of one and two cracks—schematic representation.

$$\begin{Bmatrix} {}^{i}N_{xx} \\ {}^{i}M_{xx} \end{Bmatrix} = \begin{bmatrix} {}^{i}A_{11} & {}^{i}B_{11} \\ {}^{i}B_{11} & {}^{i}D_{11} \end{bmatrix} \begin{Bmatrix} {}^{i}\varepsilon_{xx} \\ {}^{i}k_{xx} \end{Bmatrix}, \tag{3}$$

$$({}^{i}A_{jk}; {}^{i}B_{jk}; {}^{i}D_{jk}) = b \int_{z} {}^{i}Q_{jk}(1, z, z^2)\, \mathrm{d}z, \tag{4}$$

where ${}^{i}N_{xx}$, ${}^{i}M_{xx}$ respectively are the axial force and bending moment of region i, b strip width and Q_{jk} the laminate transformed reduced stiffnesses.

When the width-to-span ratio is large, the lateral stiffness parameters affect the unidirectional terms and the cylindrical bending theory must be applied. In that case, only $\varepsilon_{yy} = 0$, $k_{yy} = 0$, are imposed and the constitutive equations read:

$$\begin{Bmatrix} {}^{i}N_{xx} \\ {}^{i}N_{xy} \\ {}^{i}M_{xx} \\ {}^{i}M_{xy} \end{Bmatrix} = \begin{bmatrix} {}^{i}A_{11} & {}^{i}A_{16} & {}^{i}B_{11} & {}^{i}B_{16} \\ & {}^{i}A_{22} & {}^{i}B_{16} & {}^{i}B_{22} \\ & & {}^{i}D_{11} & {}^{i}D_{16} \\ \text{symm.} & & & {}^{i}D_{66} \end{bmatrix} \begin{Bmatrix} {}^{i}\varepsilon_{xx} \\ {}^{i}\gamma_{xy} \\ {}^{i}k_{xx} \\ {}^{i}k_{xy} \end{Bmatrix}, \tag{5}$$

with the lateral forces defined as:

$$\begin{Bmatrix} {}^{i}N_{yy} \\ {}^{i}M_{yy} \end{Bmatrix} = \begin{bmatrix} {}^{i}A_{21} & {}^{i}A_{22} & {}^{i}B_{21} & {}^{i}B_{22} \\ {}^{i}B_{21} & {}^{i}B_{22} & {}^{i}D_{21} & {}^{i}D_{22} \end{bmatrix} \begin{Bmatrix} {}^{i}\varepsilon_{xx} \\ {}^{i}\gamma_{xy} \\ {}^{i}k_{xx} \\ {}^{i}k_{xy} \end{Bmatrix}. \tag{6}$$

For the one-dimensional case, expressing the strain in terms of the axial force and substituting it for the bending moment [see Sheinman (1989)], we have:

$$\begin{aligned} {}^{i}N_{xx} &= {}^{i}A_{11}{}^{i}\varepsilon_{xx} + {}^{i}B_{11}{}^{i}k_{xx}, \\ {}^{i}M_{xx} &= {}^{i}b_{11}{}^{i}N_{xx} + {}^{i}d_{11}{}^{i}k_{xx}, \end{aligned} \tag{7}$$

where

$${}^{i}b_{11} = \frac{{}^{i}B_{11}{}^{i}A_{66} - {}^{i}B_{16}{}^{i}A_{16}}{{}^{i}A_{11}{}^{i}A_{66} - {}^{i}A_{16}^2}, \tag{8}$$

$${}^{i}d_{11} = D_{11} - \frac{({}^{i}B_{11})^2{}^{i}A_{66} - 2{}^{i}B_{11}{}^{i}A_{16} + ({}^{i}B_{16})^2{}^{i}A_{11}}{{}^{i}A_{11}{}^{i}A_{66} - ({}^{i}A_{16})^2}. \tag{9}$$

It should be noted that while ${}^{i}A_{11}$ and ${}^{i}B_{11}$ are functions of the z-coordinate alone, the bending coefficients ${}^{i}b_{11}$ and ${}^{i}d_{11}$ are functions of the lateral direction as well, expressed by A_{16}, A_{66} and B_{16}. It can also be seen that the cylindrical bending stiffness d_{11} is always smaller compared with its beam theory counterpart. Finally, since the above procedure is not consistent (the terms representing shear and torsion [eqn (5)] are not zero along the edges of the beam) the axial-bending coupling coefficient differs from the bending axial one (asymmetry). However, from the engineering point of view, the results are applicable and close to those of two-dimensional theory [see Soffer (1989)].

Equilibrium equations

Resorting to the variational principle, the following non-linear equations are obtained for each region i:

$$
\begin{aligned}
{}^{i}N_{xx,x} &= -{}^{i}q_x, \\
{}^{i}M_{xx,xx} + [{}^{i}N_{xx}({}^{i}w_{,x} + {}^{i}\bar{w}_{,x})]_{,x} &= -{}^{i}q_z,
\end{aligned} \tag{10}
$$

where q_x and q_z (function of x) are the external axial and transverse loadings, respectively.

The boundary conditions are as follows:

$$
\begin{aligned}
{}^{i}u - ({}^{i}z_{\text{sup}} - {}^{i}z_{\text{ref}}){}^{i}w_{,x}\big|_{x=0}^{x=l} &= {}^{i}u^* \quad \text{or} \quad {}^{i}N^*, \\
{}^{i}w\big|_{x=0}^{x=l} &= {}^{i}w^* \quad \text{or} \quad {}^{i}M_{xx,x} + {}^{i}N_{xx}{}^{i}w_{,x}\big|_{x=0}^{x=l} = {}^{i}S^*, \\
{}^{i}w_{,x}\big|_{x=0}^{x=l} &= {}^{i}w^*_{,x} \quad \text{or} \quad {}^{i}M_{xx} - {}^{i}N_{xx}({}^{i}z_{\text{sup}} - {}^{i}z_{\text{ref}})\big|_{x=0}^{x=l} = {}^{i}M^*,
\end{aligned} \tag{11}
$$

where ${}^{i}u^*$, ${}^{i}w^*$ and ${}^{i}w^*_{,x}$ are the external applied displacements and ${}^{i}N^*$, ${}^{i}S^*$ and ${}^{i}M^*$ are the external applied forces at the boundaries.

At the crack tips the following displacement and rotation compatibility equations (per joint) are imposed [see Sheinman and Soffer (1991)]:

$$
\begin{aligned}
{}^{1}u + {}^{1}z_{\text{ref}}{}^{1}w_{,x} = {}^{2}u + {}^{2}z_{\text{ref}}{}^{2}w_{,x} = \cdots = {}^{n}u + {}^{n}z_{\text{ref}}{}^{n}w_{,x}, \\
{}^{1}w = {}^{2}w = \cdots = {}^{n}w, \\
{}^{1}w_{,x} = {}^{2}w_{,x} = \cdots = {}^{n}w_{,x};
\end{aligned} \tag{12}
$$

and the following force compatibility equations:

$$
\begin{aligned}
\sum_{k=1}^{n} N_{xx}^{k} &= 0, \\
\sum_{k=1}^{n} (M_{xx,x} + N_{xx}(w_{,x} + \bar{w}_{,x}))^{k} &= 0, \\
\sum_{k=1}^{n} (M_{xx} - N_{xx}z_{\text{ref}})^{k} &= 0,
\end{aligned} \tag{13}
$$

where n is the number of members branching from the joint.

3. SOLUTION PROCEDURE

The non-linear behavior can be found by shifting the reference surface in each sublaminate to ${}^{i}z_{\text{ref}} = {}^{i}z + {}^{i}e$, such that the equation

$$
{}^{i}b_{11}({}^{i}z_{\text{ref}}) = 0, \quad i = 1, 2, \ldots, m, \tag{14}
$$

is satisfied, ${}^{i}z$ being the z-coordinate of the median axis and ${}^{i}e$ an eccentricity given by:

$$
{}^{i}e = -{}^{i}b_{11}({}^{i}z)/{}^{i}A_{11}({}^{i}z). \tag{15}
$$

The non-linear partial differential equilibrium [eqn (10)], compatibility [eqns (12), (13)] and boundary [eqn (11)] equations are first written in terms of displacements and then replaced by a sequence of algebraic non-linear ones by discretization of the unknown displacement functions into truncated known series. The characteristic eigenfunctions of the buckling equation of a multiply delaminated structure [see Adan *et al.* (1993)] are taken as a natural basis for the series. The jth eigenfunction for region i in the axial and transverse directions, respectively, can be written as:

$$
\begin{aligned}
{}^{i}e_j(\xi) &= [{}^{i}C_1 + {}^{i}C_2\xi]_j, \\
{}^{i}f_j(\xi) &= [{}^{i}C_3 + {}^{i}C_4\xi + {}^{i}C_5 \sin({}^{i}\beta\xi) + {}^{i}C_6 \cos({}^{i}\beta\xi)]_j,
\end{aligned} \tag{16}
$$

where $\xi = x/l$ is the non-dimensional axial coordinate, β and C_l are the characteristic parameters, determined through the boundary condition at $\xi = 0$ and $\xi = 1$. In the non-linear analysis, the axial and transverse displacements are coupled through the non-linear term of eqn (2), and the functions of eqns (16) do not satisfy the force conditions. Accordingly, additional non-linear functions should be introduced for the displacement. In the absence of consistent analytical means for finding such compatible functions, a systematic guesswork procedure is resorted to. A schematic description of the characteristic global and local approach displacement functions is given in Fig. 3 for a clamped–simply-supported delaminated beam model. The transverse displacement is represented in the figure by the mode shapes, and the axial displacement by its ordinates. Figure 3(a) shows the delaminated model; 3(b) the global buckling eigenfunctions of the axial (${}^ie_j$) and transverse (${}^if_j$) displacements; 3(c) the local transverse functions (likewise in terms of ${}^if_j$) subject to the non-linear force continuity conditions; 3(d) the global axial displacements; 3(e) the local axial displacements. The local functions are defined separately for each region, with the same sequence numbering as for the global ones. Thus the axial, transverse and imperfection displacements can be written as:

$$
\begin{aligned}
{}^iu(\xi) &= \sum_{j=0}^{Nu} u_j\,{}^ig_j(\xi) + \sum_{j=1}^{Nw} w_j\,{}^ie_j(\xi),\\
{}^iw(\xi) &= \sum_{j=1}^{Nw} w_j\,{}^if_j(\xi),\\
{}^i\bar{w}(\xi) &= \sum_{j=1}^{Nw} \bar{w}_j\,{}^if_j(\xi),
\end{aligned}
\tag{17}
$$

where u_j, w_j and w_j are the unknown scalars written in global form; Nu, Nw are the truncated number of the u- and w-series functions; ${}^ie_j$, which contains only global functions, is the axial component of the buckling eigenfunctions; g_j is composed of global linear functions ${}^ig_0(\xi) = \xi$ for a moving support on the right-hand side or $= 1-\xi$ for a moving

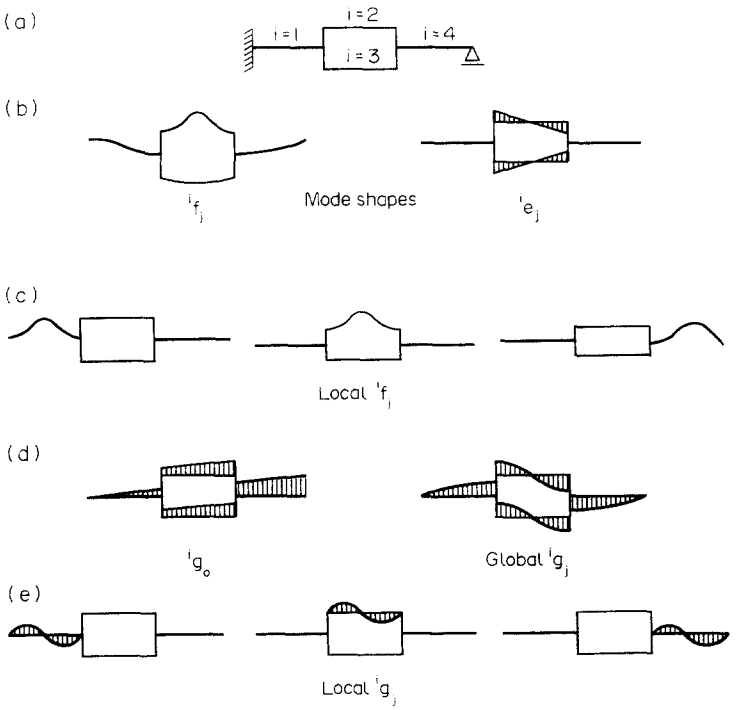

Fig. 3. Global and local displacement approximation functions: (a) geometrical model; (b) buckling mode functions; (c) transverse displacement local functions; (d) axial displacement global functions; (e) axial displacement local functions.

support on the left-hand side, and of global and local non-linear functions derived from the Airy stress function; f_j is composed of global functions which are the transverse components of the buckling eigenfunctions and of the local transverse functions.

The global functions of u and w, by their definitions, automatically satisfy the essential continuity and boundary conditions. For the local functions, a strong form ensuring that each one of them satisfies exactly the essential conditions, is adopted. Thus, while the displacement continuity and boundary conditions are satisfied directly for each single function, the force condition is accommodated gradually in a convergence procedure with respect to the number of truncated series functions.

The additional global and local functions for axial displacement (${}^{i}g_j$), which are derived through integration of the Airy stress function [see Sheinman *et al.* (1993)], can be written, for any i-region, in terms of the global ξ-coordinate, as:

$$ {}^{i}g_j(\xi) = \xi - \frac{{}^{i}\xi_r - {}^{i}\xi_l}{\alpha_j}\left[\sin\left(\alpha_j \frac{\xi - {}^{i}\xi_l}{{}^{i}\xi_r - {}^{i}\xi_l}\right) + \gamma_j \cos\left(\alpha_j \frac{\xi - {}^{i}\xi_l}{{}^{i}\xi_r - {}^{i}\xi_l}\right)\right] - \frac{\alpha_j \gamma_j}{{}^{i}\xi_r - {}^{i}\xi_l}\left(\tfrac{1}{2}\xi^2 - \xi\,{}^{i}\xi_l\right) + \frac{\gamma_j}{\alpha_j}, $$

$$ \gamma_j = (\cos\alpha_j - 1)/(\sin\alpha_j - \alpha_j), \quad {}^{i}\xi_l \leqslant \xi \leqslant {}^{i}\xi_r, \tag{18} $$

where ${}^{i}\xi_l$ and ${}^{i}\xi_r$ are the coordinates of region i for the local functions, for the global functions, ${}^{i}\xi_l = 0$, ${}^{i}\xi_r = 1$ and α_j are the characteristic roots derived from:

$$ \sin\frac{\alpha_j}{2}\left(\tan\frac{\alpha_j}{2} - \frac{\alpha_j}{2}\right) = 0. \tag{19} $$

Two different kinds of displacement families are observed: the symmetric function [see Sheinman *et al.* (1993)] for which α_j is determined from $\tan(\alpha_j/2) - (\alpha_j/2) = 0$, $j = 2, 4, 6, \ldots$, with $\gamma_j \neq 0$, and the asymmetric ones for

$$ \alpha = (j+1)\pi \text{ determined from } \sin\frac{\alpha_j}{2} = 0 \quad \text{with } \gamma_j = 0. $$

It should be noted that ${}^{i}g_j$ is defined for one region at a time (for all other regions ${}^{i}g_j = 0$). Thus, it is obvious from the essential displacement conditions that g_j should be zero at the boundaries $\xi = {}^{i}\xi_l$ and $\xi = {}^{i}\xi_r$. The integration coefficient γ_j/α_j [see eqn (18)] zeros the function at $\xi = {}^{i}\xi_l$. The value at the right-hand boundary is zero for the symmetric functions [Fig. 4(a)] and non-zero for the asymmetric ones [Fig. 4(b)]. This problem can

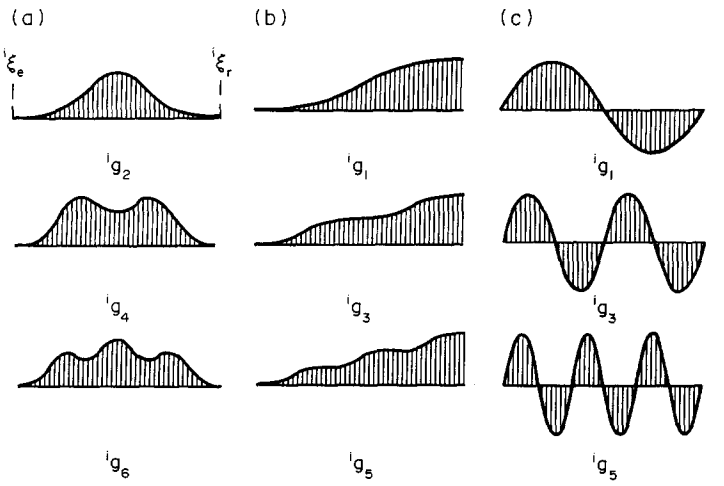

Fig. 4. Axial displacement approximation functions ${}^{i}g_j$ (a) symmetric; (b) asymmetric; (c) anti-symmetric.

be resolved, without detracting from its generality, by omitting the linear terms from the asymmetric formula, thus:

$$ {}^{i}g_j(\xi) = \sin\left((j+1)\pi\frac{\xi - {}^{i}\xi_1}{{}^{i}\xi_r - {}^{i}\xi_1}\right), \quad j = 1,3,5,\ldots, \tag{20} $$

as shown in Fig. 4(c).

The local transverse displacement functions are chosen to be of the same type as the global ones, namely:

$$ {}^{i}f_j(\xi) = \left[{}^{i}C_3 + {}^{i}C_4\frac{\xi - {}^{i}\xi_1}{{}^{i}\xi_r - {}^{i}\xi_1} + {}^{i}C_5\sin\left({}^{i}\beta\frac{\xi - {}^{i}\xi_1}{{}^{i}\xi_r - {}^{i}\xi_1}\right) + {}^{i}C_6\cos\left({}^{i}\beta\frac{\xi - {}^{i}\xi_1}{{}^{i}\xi_r - {}^{i}\xi_1}\right)\right]_j, \quad {}^{i}\xi_1 \leqslant \xi \leqslant {}^{i}\xi_r. \tag{21} $$

Here, ${}^{i}\beta$ and ${}^{i}C_1$ are determined through the end conditions of the local region i. Since the procedure is designed so that the local functions in region i do not affect any other region, conditions of the clamped–clamped type are introduced for any internal region. For the end regions the same given global boundary conditions are imposed on the local functions.

Equation (21) can be rewritten in compact form as

$$ {}^{i}f_j(\xi) = [{}^{i}\bar{C}_3 + {}^{i}\bar{C}_4\xi + {}^{i}\bar{C}_5\sin({}^{i}\bar{\beta}\xi) + {}^{i}\bar{C}_6\cos({}^{i}\bar{\beta}\xi)]_j, \tag{22} $$

with

$$ \begin{aligned} {}^{i}\bar{\beta} &= {}^{i}\beta/({}^{i}\xi_r - {}^{i}\xi_1), \\ {}^{i}\bar{C}_3 &= {}^{i}C_3 - {}^{i}C_4{}^{i}\xi_1/({}^{i}\xi_r - {}^{i}\xi_1), \\ {}^{i}\bar{C}_4 &= {}^{i}C_4/({}^{i}\xi_r - {}^{i}\xi_1), \\ {}^{i}\bar{C}_5 &= {}^{i}C_5\cos({}^{i}\bar{\beta}\,{}^{i}\xi_1) + {}^{i}C_6\sin({}^{i}\bar{\beta}\,{}^{i}\xi_1), \\ {}^{i}\bar{C}_6 &= -{}^{i}C_5\sin({}^{i}\bar{\beta}\,{}^{i}\xi_1) + {}^{i}C_6\cos({}^{i}\bar{\beta}\,{}^{i}\xi_1). \end{aligned} \tag{23} $$

The above procedure yields a non-linear algebraic system, characterized by limit-point behavior involving snap-buckling, rather than by bifurcation points. Accordingly, a modified "arc-length" method [see Riks (1979) and Adan (1991)] and the Newton–Raphson procedure are applied to solve the system for a given number of functions in the truncated series.

4. NUMERICAL RESULTS AND DISCUSSION

A general computer code NAMDL (Nonlinear Analysis of Multiply Delaminated Laminates) was developed for the procedure outlined above. It is suitable for laminated beams with an arbitrary number of delaminations and any stacking combination. A realistic picture has to include contact constraints, but as the appropriate algorithm is still in the basic stage of investigation [see Adan *et al.* (1993)], the present analysis is confined to situations not involving the contact effect which can in some cases be tackled with the aid of appropriate imperfection shapes. Examples of simply-supported beams under axial compression are considered below.

The first example involving a single delamination, illustrates the proposed approach versus the finite-difference method by Sheinman and Soffer (1991). The beam data are: span $l = 4.0$ m; width $b = 0.04$ m; total depth $h = 0.08$ m, thickness of delaminated upper layer $t_1 = h/8 = 0.01$ m; delamination at midspan $d_1 = 0$ (see Fig. 1); delamination length $2a_1 = 3l/8 = 1.50$ m; modulus of elasticity $E = 210$ GPa N m^{-2}, Poisson's ratio $\nu = 0.3$. The initial imperfection was taken, in order to obviate the contact effect, as $\bar{w}(\xi) = -0.0001\sin\pi\xi$ over the entire beam span. For the transverse displacement 8 global

and 6 local functions (see Fig. 5) were taken into account. Similarity of some of the local and global shapes [such as ${}^1f_1$ and ${}^1f_9$, ${}^if_3$ and ${}^if_{10}$, ${}^if_4$ and ${}^if_{11}$ (Fig. 5)] is confined to the local region, the global functions reflect the bending of the structure as a whole. The initial imperfection was applied through the first and second global functions.

For the axial displacement 18 functions were considered as follows: 4 global functions—one linear $g_0(\xi) = \xi$ and three asymmetric [eqn (20)], and 14 local functions (symmetric and asymmetric for regions 1 and 4 respectively, [see Fig. (6)], seven asymmetric functions for the buckled stretch $i = 2$ and three asymmetric ones for region 3). The large number of approximated local functions in the buckled stretch is needed for satisfying the non-linear compatibility equations. In the regions of symmetric bending $i = 2$ and $i = 3$, only the asymmetric axial functions are relevant. The load–deflection curves for all regions (i), are plotted in Fig. (6) versus finite difference method. In this figure $\bar{N}_{\text{perf}}$ is the axial load of a perfect undelaminated structure. At $\bar{N} = N/N_{\text{perf}} = 0.42$ local buckling of region 2, followed by global bending is observed. With further increase of the axial load, the behavior becomes highly non-linear, asymptotic to the ultimate load capacity $\bar{N} = 0.76$. The overall behavior, composed of local buckling followed by global bending, is expressed in the plots of w_j and u_j shown in Figs 7(a) and 7(b), respectively, with the solid lines representing global functions and the dashed lines, local functions. It is seen that only seven functions, four global and three local, are affected. ${}^if_2$ describes the overall behavior while the others

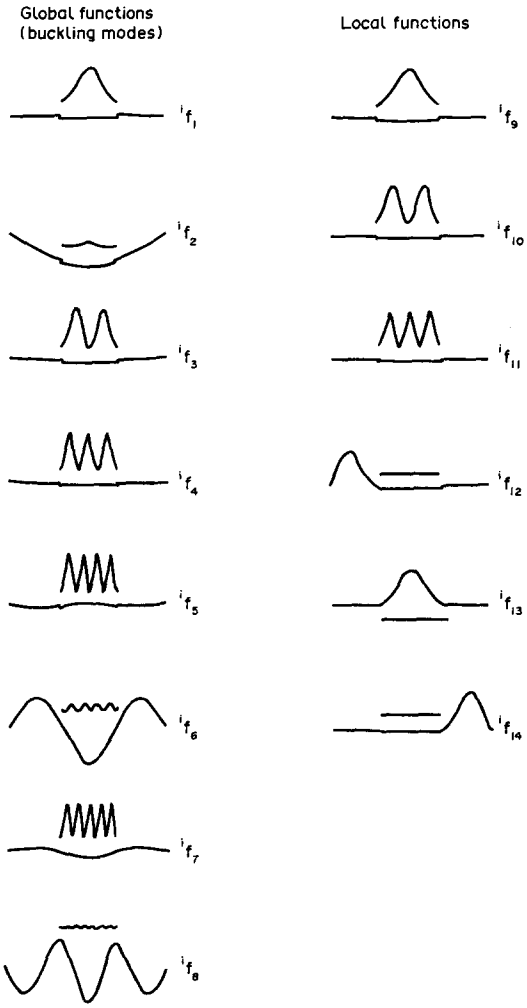

Fig. 5. Transverse displacement approximation functions for numerical example 1 (single delamination).

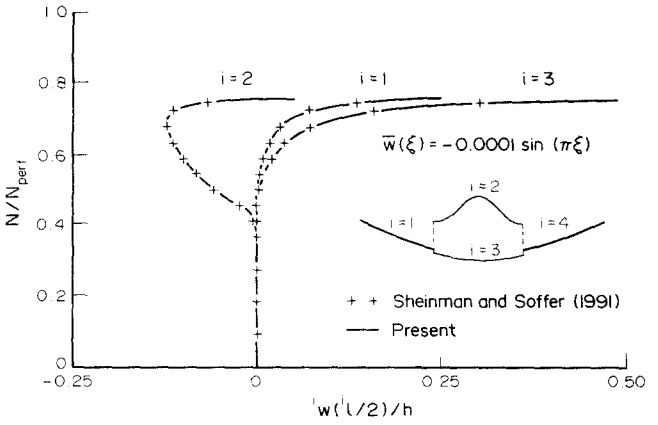

Fig. 6. Load–displacement curves for example 1.

contribute to the local ones. The contribution of the wavelength functions ${}^{i}f_1$ and ${}^{i}f_9$ to the behavior [see Fig. 7(a)], are the most predominant, and the higher the load level, the higher wavelength functions are (f_3, f_{10}, f_4, f_{11}). In the zoom area it is clearly seen that the initial buckling behavior (at $N = 0.442$) is affected by f_1 and f_9 only. With further increase of the axial load, additional local functions are affected. At $N = 0.52$ global bending is observed. From Fig. 7(b) one can see that the linear axial function, by which the axial load is dictated,

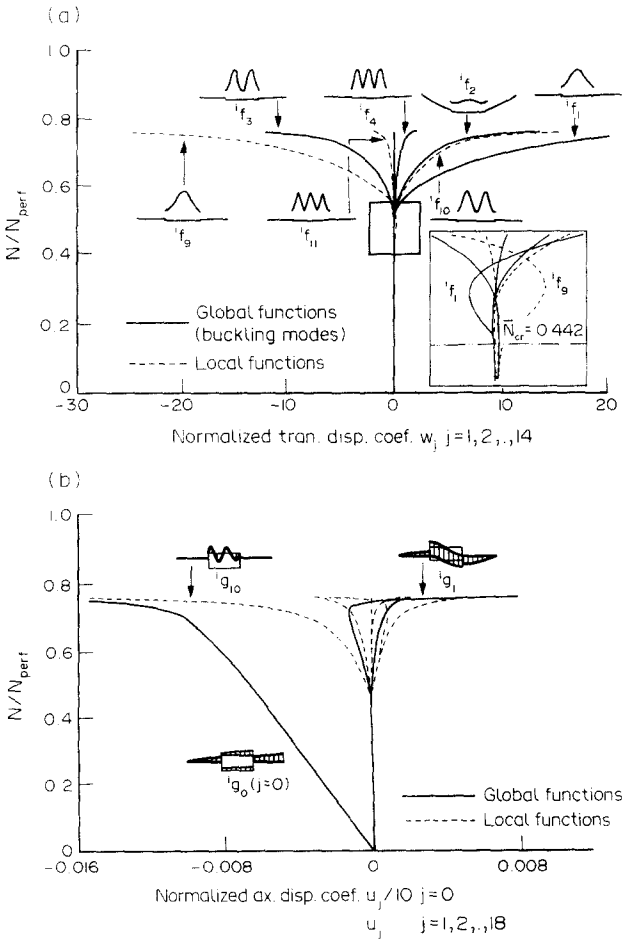

Fig. 7. Variation of coefficients of approximation functions with respect to load level: (a) transverse displacement w_j; (b) axial displacement u_j.

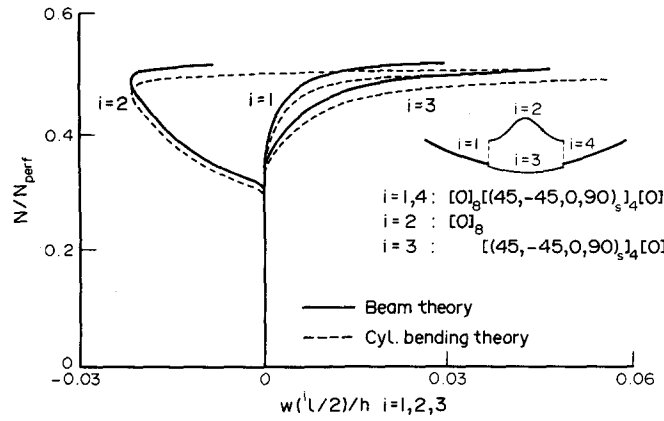

Fig. 8. Load–displacement curve of anisotropic beam with single delamination.

is the dominant parameter up to the local buckling point, beyond which non-linear behavior sets in. (Note that this function is scaled by 10 for comparison with the effect of the functions.) In the post-buckling area g_1 and g_{10} become pronounced. Nonlinear compatibility of the force equations is satisfied by incorporating the local functions. Although their effect is not as high as that of the others, without considering them the solution does not converge.

The effect of cylindrical buckling was studied on the anisotropic delaminated beam reproduced from Sheinman and Soffer (1991) and described in Fig. 8. The anisotropic properties are given only for region $i = 3$ for which $A_{16} = B_{16} = D_{16} = 0$ due to its balanced sequence. Thus the constitutive relations of bending theory [eqn (3)] and cylindrical bending theory [eqns (8) and (9)] are the same. For the lateral direction, another type: $b_{11} = (A^{-1}B)_{11}$, $d_{11} = D_{11} - (BA^{-1}B)_{11}$ was considered. For comparison, a more accurate model [see Soffer (1989)] of plate elements was run using the general-purpose finite element NASTRAN code. The results of the present one-dimensional algorithm, with the lateral effect taken into account through d_{11}, are the same as those of the NASTRAN two-dimensional model.

The second example is concerned with a multiply delaminated beam (two cracks). Data: simply-supported boundary conditions, span $l = 4.0$ m, thickness $h = 0.08$ m, modulus of elasticity $E = 210$ GPa N m^{-2}, Poisson's ratio $v = 0.3$, delamination length $2a_1 = 2a_2 = 1.5$ m, delamination depth (see Fig. 1) $t_1 = 0.01$ m, $t_2 = 0.02$ m, location $d_1 = 0$, $d_2 = 0.75$ m. This location was chosen so as to yield the minimum classical buckling load, the right-hand boundary of the upper sublaminate is connected to the most flexible point of its lower counterpart [see Adan *et al.* (1993)]. In this case 25 functions were used for transverse displacement and 37 for axial displacement. The large number of terms was necessary for the asymmetric bending due to the larger number of segments in the model. Here, the imperfection was taken only in the upper sublaminate ($i = 2$) with amplitude -1.10^{-3} m. The axial load versus transverse displacement for three different points (A, B and C) is given in Fig. 9. Solution convergence was slow because of the need to satisfy the non-linear compatibility requirement in regions 2 and 4 (at the ends of which the Gibbs phenomenon was observed). At $\bar{N} = N/N_{\text{perf}} = 0.406$ the upper sublaminate buckled (as against 0.442 for a single crack). Increase of the axial load caused downward bending and the ultimate load capacity is $\bar{N} = 0.7$ (as against $\bar{N} = 0.77$ for a single crack). Somewhere around $\bar{N} = 0.58$ the second sublaminate buckles and the total capacity is reduced from 0.77 to 0.7.

5. CONCLUSION

Post-buckling analysis of a beam with arbitrary multiple delaminations is presented, using a one-dimensional model. The delaminations divide the beam into regions, for each of which non-linear equilibrium equations based on the Von Karman kinematic approach

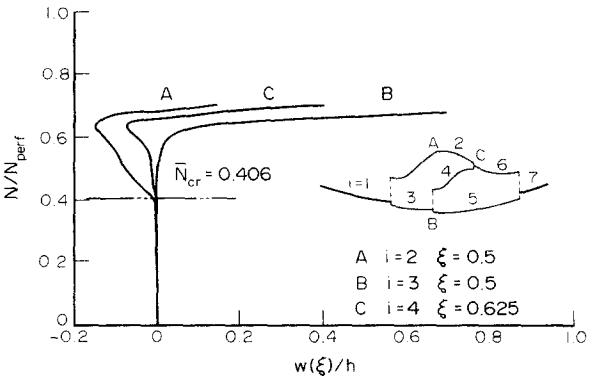

Fig. 9. Load–displacement curves for beam with two delaminations.

are applied. In addition, displacement and force continuity conditions are imposed at the crack tips. The partial differential equations are converted into a sequence of algebraic ones by variable separation, using global and local functions. The most difficult problem, satisfying non-linear force compatibility at the crack tips, was successfully solved by introducing special local functions in the transverse and axial directions. Although large numbers of functions are needed to complete the solution, convergence is much better than for the numerical finite-difference or finite-element methods. The theory and solution procedure are general and suitable for investigating the effect of multiple delaminations on the overall non-linear behavior. The classical buckling load provides only an indication of the picture, and post-buckling analysis is called for. The procedure permits inclusion of the contact constraints for more realistic delamination cases.

Acknowledgements—The study was financed in part by the VPR Foundation of the Technion. The authors are indebted to Ing. E. Goldberg for editorial assistance.

REFERENCES

Adan, M. (1991). Buckling of multiply delaminated composite laminates. D.Sc. thesis, Technion-IIT, ISRAEL (in Hebrew, English summary).

Adan, M., Sheinman, I. and Altus, E. (1993). Buckling of multiply delaminated laminates. Submitted for publication.

Bolotin, V. V., Zebel'yan, Z. Kh. and Kurzin, A. A. (1980). Stability of compressed components with delamination type flaws. *Probl. Proch.* **7**, 813–819.

Chai, H., Babcock, G. D. and Knauss, W. G. (1981). One-dimensional modeling of failure in laminated plates by delamination buckling. *Int. J. Solids Structures* **17**, 1069–1083.

Chang, F. K. and Kutlu, Z. (1989). Collapse analysis of composite panels with multiple delamination. *Proc. 30th AIAA/ASME/ASCE/AHS/ASC SDM Conf.*, Alabama, pp. 989–999.

Larsson, P. L. (1991). On multiple delamination buckling and growth in composite plates. *Int. J. Solids Structures* **27**, 1623–1637.

Riks, E. (1979). An incremental approach to the solution of snapping and buckling problems. *Int. J. Solids Structures* **15**, 529–551.

Sheinman, I. (1989). Cylindrical buckling load of laminated columns. *ASCE J. Engng Mech.* **115**(3), 659–661.

Sheinman, I., Adan, M. and Altus, E. (1993). On the role of the displacement function in nonlinear analysis of beams. *Thin Walled Structures* (to appear).

Sheinman, I., Bass, M. and Ishai, O. (1989). Effect of delamination on stability of laminated composite strip. *J. Compos. Struct.* **11**, 227–242.

Sheinman, I. and Soffer, M. (1991). Post-buckling analysis of composite delaminated beams. *Int. J. Solids Structures* **27**, 639–646.

Shivakumar, K. N. and Whitcomb, J. D. (1985). Buckling of sublaminate in a quasi-isotropic composite laminate. *J. Compos. Mater.* **19**, 2–18.

Simitses, G. J., Sallam, S. and Yin, W. L. (1985). Effect of delamination of axially loaded homogeneous laminated plate. *AIAA Jl* **23**(9), 1437–1444.

Soffer, M. (1989). The effect of delamination on the non-linear behavior of composite laminated beams. M.Sc thesis Technion-IIT, ISRAEL (in Hebrew, English summary).

Yin, W. L. (1986). Cylindrical buckling of laminated and delaminated plates. *Proc. 27th AIAA/ASME/ASCE/AHS/ASC SDM Conf. Part 1* San Antonio, TX, pp. 165–179.

Yin, W. L., Sallam, S. and Simitses, G. J. (1984). Ultimate axial load capacity of delaminated plate. *Proc. 25th AIAA/ASME/ASCE/AHS/ASC SDM Conf.* paper 84-08-92 Palm Springs, CA.